Available online at www.sciencedirect.com

ScienceDirect

Chronic Diseases and Translational Medicine 2 (2016) 159–165

www.keaipublishing.com/en/journals/cdtm/

www.cdatm.org

Original Article

# Coronary artery plaque imaging: Comparison of black-blood MRI and 64-multidetector computed tomography

Yi He [a], Qin-Yi Da [a], Jing An [b], Xian-Tao Song [c,*], De-Biao Li [d]

[a] *Department of Radiology, Beijing Institute of Heart, Lung and Blood Vessel Disease, Beijing Anzhen Hospital, Capital Medical University, Beijing 100029, China*

[b] *Siemens Healthcare, MR Collaboration NE Asia, Beijing 100102, China*

[c] *Department of Cardiology, Beijing Institute of Heart, Lung and Blood Vessel Disease, Beijing Anzhen Hospital, Capital Medical University, Beijing 100029, China*

[d] *Cedars-Sinai Medical Center, University of California, Los Angeles, USA*

Received 17 September 2016

Available online 3 December 2016

## Abstract

**Objective:** To comparatively evaluate black-blood coronary arterial wall MRI and 64-multidetector computed tomography (64-MDCT) for detection and classification of coronary artery plaques.

**Methods:** We included 15 patients with confirmed coronary artery plaques in the proximal or middle segments of coronary arteries by 64-MDCT, who underwent black-blood coronary wall MRI at 1.5 T within 10 days. Cross-sectional coronary wall images were acquired using a 2D double-inversion-recovery, electrocardiograph-triggered, navigator-gated, fat-suppressed, turbo-spin-echo sequence on the coronary arteries with lesions from the ostium to the middle segment continuously without gap. The vessel cross-sectional area (CSA), luminal CSA, maximal wall thickness, plaque burden, contrast-to-noise ratio (CNR), and signal-to-noise ratio (SNR) were measured in each slice and subsequently compared with computed tomography angiography (CTA) images. CTA images were divided into 5-mm segments for side-by-side comparison with MRI.

**Results:** Of the 15 patients, 12 were enrolled in the study. Coronary plaques were found in 46 slices on both CTA and MRI. Plaques were classified to 3 groups based on CTA: calcified plaques ($n = 11$), soft plaques ($n = 23$), and mixed plaques ($n = 12$). In MRI, the plaque burden, maximal wall thickness, SNR, and CNR in the coronary walls containing plaques were greater than in the normal coronary walls ($0.83 \pm 0.08$ *vs.* $0.73 \pm 0.08$, $1.88 \pm 0.51$ *vs.* $1.51 \pm 0.26$ mm, $12.95 \pm 2.78$ *vs.* $9.93 \pm 2.31$, and $6.76 \pm 2.52$ *vs.* $3.89 \pm 1.54$, respectively; $P < 0.05$). The luminal CSA at the plaque was smaller than in normal coronary walls ($2.50 \pm 1.50$ *vs.* $4.72 \pm 2.28$ mm$^2$; $P < 0.05$). The SNR in the soft plaque was significantly greater than in calcified and mixed plaques ($P < 0.05$).

**Conclusions:** Coronary wall MRI can identify coronary plaques in the proximal and middle segments and has the potential to differentiate plaque types based on signal intensity.

* Corresponding author.

*E-mail address:* songxiantao@medmail.com.cn (X.-T. Song).

Peer review under responsibility of Chinese Medical Association.

Production and Hosting by Elsevier on behalf of KeAi

http://dx.doi.org/10.1016/j.cdtm.2016.11.007

*Keywords:* Magnetic resonance imaging; Coronary artery; Wall imaging; Atherosclerosis; Plaques

## Introduction

Coronary atherosclerotic plaque rupture is the most common plaque complication, accounting for most cases of fatal acute myocardial syndrome. Several investigations indicated that plaque composition, plaque burden, and progression of coronary atherosclerosis were important risk factors for adverse coronary events.[1–3] Therefore, identifying rupture-prone vulnerable plaque is important for preventing an acute coronary event.

Imaging tools such as intravascular ultrasound (IVUS) and optical coherence tomography (OCT) reliably determine plaque burden and plaque composition. However, IVUS and OCT are invasive and unsuitable for routine applications related to risk stratification. Multidetector computed tomography (MDCT) is suitable for non-invasive detection and quantification of calcified coronary plaques, but it has limited ability to identify the composition of non-calcified plaques because of the pool contrast-to-noise ratio (CNR) in soft tissues.[4] Studies have suggested the potential of high-resolution black blood coronary arterial wall MRI for assessment of coronary artery wall thickness[5–7] and non-invasive measurement of plaque burden and remodeling[8]; however, systematic MRI-evaluation of coronary plaque components and morphology has not been conducted previously. The purpose of this study was to evaluate the ability of black-blood coronary arterial wall MRI to identify and classify coronary artery plaques by comparing with 64-MDCT.

## Materials and methods

### *Patients*

From May 2009 to November 2009, 15 patients (mean age 56 ± 12 years, 10 men) with confirmed coronary artery plaques in the proximal or middle segments of coronary arteries by 64-MDCT were recruited in our study. Exclusion criteria were acute myocardial infarction (MI) within 2 weeks, unstable angina, heart rate >80 beats/min, post percutaneous coronary intervention (PCI) or coronary artery bypass grafting (CABG), arrhythmia, and any contraindications to MR examination (metallic implants such as pacemakers, defibrillators, cerebral aneurysm clips, severe claustrophobia). All patients underwent MR scan within 10 days of MDCT. Written informed consent was obtained from each patient. All persons gave their informed consent prior to inclusion in the study.

### *MRI protocol*

All participants were imaged on a 1.5-T whole-body magnetic resonance scanner (Sonata, Siemens, Erlangen, Germany) with a gradient strength of 40 mT/m, slew rate of 200 $T \cdot m^{-1} \cdot s^{-1}$, and 12-channel receive coils (6 anterior and 6 posterior). The R-wave acquired from a 4-lead electrocardiograph (ECG) was used to trigger the data acquisition. An elastic belt was placed on the abdomen of the patient to avoid changes in depth of breathing during data acquisition. β-blocker (25–50 mg) was given orally to patients with heart rate >75 beats/min. All images were collected under free breathing with the patient in supine position.

A 4-chamber cine imaging was acquired first to determine data acquisition window (DAW). The DAW was crucial for high-quality coronary magnetic resonance angiography (MRA) and wall imaging. A free breathing, retrospective ECG-triggering steady state free precession (SSFP) sequence was used. The temporal resolution was 28 ms and spatial resolution was $2.2 \times 1.6 \times 6.0$ $mm^3$. Whole heart coronary magnetic resonance angiography (CMRA) with optional DAW provided by the cine imaging covered the entire coronary artery tree. The CMRA was acquired during free breathing using 3D ECG-triggered, navigator-gated, T2 prepared, segmented, truefast imaging with steady (TrueFISP) sequence. The sequence parameters were as follows: repetition time (TR)/echo time (TE) = 3.4/1.68 ms; bandwidth = 890 Hz/pixel; flip angle = 90°; voxel = size $0.7 \times 0.7 \times 0.9$ $mm^3$, interpolated from $1.4 \times 1.4 \times 1.5$ $mm^3$; and navigator acceptance window = ±2.5 mm.

The 3D multiplanar reformations were performed on CMRA images to show the left main coronary artery

(LM), proximal and middle left anterior descending artery (LAD), right coronary artery (RCA) and left circumflex artery (LCX). Cross-sectional coronary wall imaging was performed only on the lesion coronary artery (RCA, LM, LAD and LCX), from the ostium to the middle segment, continuously without interval. We acquired a 2D double inversion recovery, ECG-triggered navigator-gated, fat suppression, turbo spin-echo sequence with the following parameters: TR = 2R-R intervals; TE = 31 ms; echo-spacing = 6.12 ms; bandwidth = 303 Hz/pixel; matrix = 312 × 384; field of view = 400 × 325 $mm^2$; slice thickness = 5 mm; and navigator acceptance window = ±2.5 mm. Total time to complete the protocols was ≤60 min.

*MRI analysis*

Coronary wall images were graded on a 3-point scale of 1 = nonvisualization; 2 = adequate; and 3 = good.[8] Images with a score of 2 or 3 were analyzed using a software (CASCADE) at 300% zoom. The outer (adventitial) and inner (luminal) boundaries of the coronary wall were traced manually using a region-of-interest (ROI) tool. The following parameters were measured: outer contour area (vessel cross-sectional area, CSA), inner contour area (luminal CSA), and plaque burden (%) (defined as vessel cross-sectional area minus luminal cross-sectional area divided by the vessel cross-sectional area). The signal-to-noise ratio (SNR) was calculated using the following formula: $SNR = SI_{vessel\ wall}/SD_{noise}$, where SI of the vessel wall was determined by placing the ROI on the vessel wall, and the standard deviation (SD) of the background noise was determined from an ROI placed in the air anterior to the chest wall. CNR was calculated using the following formula: $CNR = (SI_{vessel\ wall} - SI_{perivascular\ area})/SD_{noise}$. For determining SI of the perivascular area, the ROI was placed in the region between the vessel wall and myocardium. The ROI was 1 $mm^2$.

*MDCT coronary angiography*

All CT examinations were performed with a 64-MDCT scanner (Aquilion, Toshiba Medical Systems, Japan). The scanning range covered the entire heart from the level of the tracheal bifurcation to the diaphragm. A 70–75 ml bolus of iopamidol (Iopamiro, Bracco, Italy) followed by 20 ml saline solution was continuously injected into an antecubital vein at a flow rate of 4.0–4.5 ml/s. Data were acquired craniocaudal with detector collimation of 64.0 × 0.5 mm thickness, gantry rotation time of 400 ms, pitch of 0.175, tube voltage of 100–135 kV, and tube current–time setting of 350–420 mAs. The entire volume of the heart was acquired during one breath-hold. Prospective or retrospective ECG gating was used.

*MDCT analysis*

The volume data of MDCT were transferred to the postprocessing workstation (Vitrea2, Version 3.8, Toshiba, Japan). Curved planar reformatting (CPR) was used to detected coronary artery plaque. Atherosclerotic plaques were considered present when the vessel wall thickness exceeded 0.5 mm. Plaques were classified into 3 groups: calcified plaques, non-calcified plaques, and mixed plaques.

*Comparison between MRI and MDCT*

For comparisons with MRI, the target coronary arteries in CTA were divided into 5-mm segments from the ostium or onset. Each 5-mm section was compared side-by-side with MRI. Side branches were selected as fiduciary points to ensure that the same corresponding coronary sections were compared. Two investigators, blinded to the results of MDCT and MRI, independently determined the presence, classification, and quantitative measurement of atherosclerotic plaque in MDCT and MRI images. Disagreement of diagnosis between the 2 readers was settled by a consensus reading.

*Statistical analysis*

All statistical analyses were performed with statistical software SPSS13.0 (SPSS Corp, College Station, NX, USA). Continuous variables were presented as means with standard deviations. Kolmogorov-Smirnov test was used for continuous variables which were normally distributed. An unpaired *t*-test was performed for differences between the coronary walls containing plaques and normal coronary walls (divided by MDCT) in MRI. A Chi-square test was used to compare difference of SNR and CNR on MRI between different types of plaque. *P* value <0.05 was considered as statistically significant.

## Results

*Participant characteristics*

The characteristics of the study population were summarized in Table 1. Three patients were

Table 1
Participant characteristics ($n = 15$).

| Items | $n$ or value |
|---|---|
| Age, years[a] | 56 ± 12 |
| Male | 10 |
| Hypertension | 5 |
| Diabetes | 4 |
| Hypercholesterol | 4 |
| Smoker | 8 |
| Chest pain | 11 |
| Family history | 6 |
| Mean heart rate, beats/min[a] | 67 ± 8 |

SD: standard deviation.
[a] Data are indicated as *mean* ± *SD*.

excluded from analysis, 2 due to poor MR image quality (patients' non-compliance due to long scan time), and 1 due to claustrophobia. Success rate was 80%. Mean heart rate was 67 ± 8 beats/min; 11 were acquired in diastole and 1 in systole. Mean navigator efficiency of whole heart MRCA was 38 ± 8, and average scan time was 664 ± 141 s. Mean navigator efficiency of wall imaging was 45 ± 12. Average scan time was 111 ± 35 s in each slice.

### *Image quality score*

A total of 74 coronary wall MRI scans with image quality scores of grades 2 and 3 from 12 participants (2 RCA, 10 LAD) were evaluated. Mean acquired slices of each vessel was 6.16. The coronary artery wall could not be visualized in 11 slices due to poor CNR, motion artifacts, and small diameter. The overall image quality scores of 74 coronary wall images were 2.65 ± 0.48. The weighted kappa value for interobserver agreement for image quality grading was 0.82.

### *Diagnostic ability of MRI coronary wall imaging*

Coronary plaques were detected in 46 of 74 slices on CTA and MRI. Plaques were classified to 3 groups based on CTA: calcified plaques ($n = 11$), soft plaques ($n = 23$), and mixed plaques ($n = 12$). In MRI, the plaque burden, maximal wall thickness, SNR, and

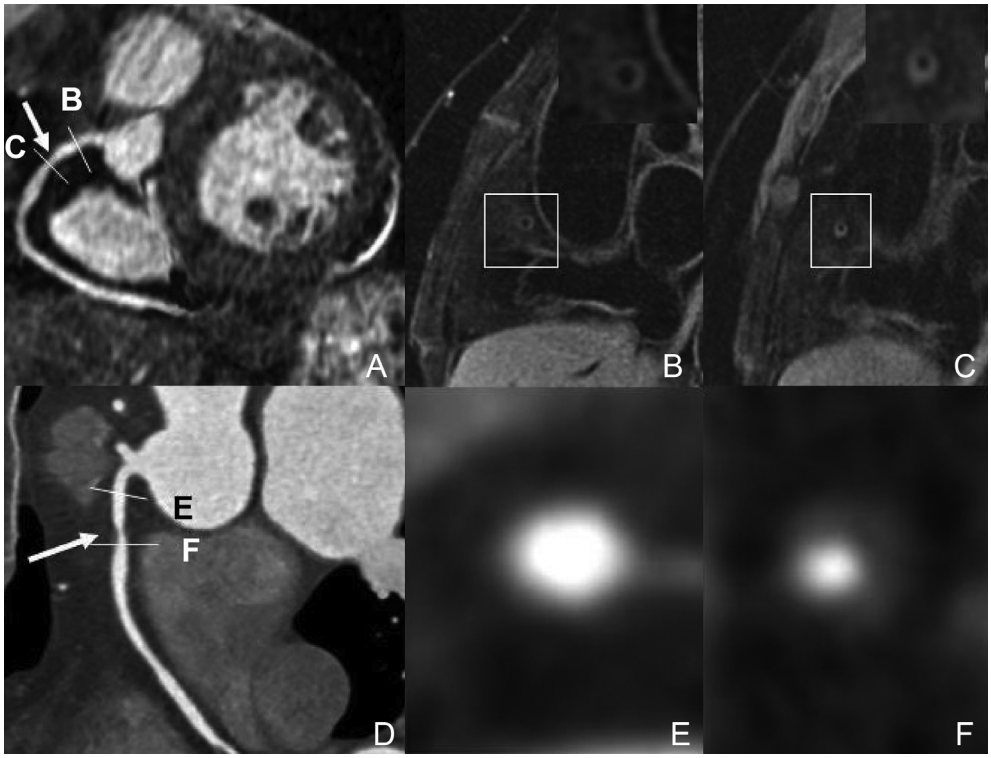


Fig. 1. Data from a 56-year-old male patient with a focal luminal stenosis in the proximal right coronary artery. A: Coronary magnetic resonance angiography. D: Multidetector computed tomography. Both show evidence of a focal non-calcified plaque (arrows) in the proximal segment of RCA. B and C demonstrate the corresponding slices in MRI. The plaque burden, maximal wall thickness, signal-to-noise ratio, and contrast-to-noise ratio in the coronary walls containing plaques were greater than those in the MRI of normal coronary walls. E and F show the cross-section in normal and plaque slice of CT.

CNR in the coronary walls containing plaques were greater than in normal coronary walls (0.83 ± 0.08 *vs.* 0.73 ± 0.08, 1.88 ± 0.51 *vs.* 1.51 ± 0.26 mm, 12.95 ± 2.78 *vs.* 9.93 ± 2.31, and 6.76 ± 2.52 *vs.* 3.89 ± 1.54, respectively, $P < 0.05$). The luminal CSA at the plaque was smaller than in normal coronary walls (2.50 ± 1.50 *vs.* 4.72 ± 2.28 $mm^2$, $P < 0.05$). The SNR in the soft plaque was significantly greater than in calcified and mixed plaques ($P < 0.05$). Fig. 1 showed coronary artery plaque in a patient. Fig. 2 showed different types of plaques.

## Discussion

In this study, we compared results from black-blood coronary wall imaging to MDCT in patients with confirmed coronary artery plaques. We used 2D double inversion recovery, ECG-triggered navigator-gated, fat suppression, and turbo spin-echo sequence for cross-section coronary artery wall imaging. In MRI imaging of coronary walls containing plaques, the plaque burden, maximal wall thickness, SNR, and CNR were significantly higher than the normal coronary walls, indicating ability of the technique to distinguish coronary artery plaque from normal walls. SNR of non-calcified plaques was higher than calcified and mixed plaque, possibly due to signal loss on calcification. This is the first study to show that MRI has the potential to identify different types of coronary plaque.

Black-blood coronary artery wall imaging was challenging because of their complex anatomical geometry, small size, heart and respiratory motion. Few previous studies reported that coronary arterial wall thickening could be found by cross-section coronary wall imaging in the patients with coronary artery disease, as compared with healthy volunteers,[5,6] whereas others reported 3D coronary wall imaging in RCA[7,9–12]; but clear 3D LAD coronary wall imaging has not been reported previously and needs to be explored. Respiration- and heartbeat-induced motion artifacts are a major challenge for CMRA. Regular respiration and heart rate are key to proper examination.[13] In this study, one case with bad image quality was caused by change in heart rate from 70 to 80 beats/min during data acquisition. In order to avoid the impact of respiratory and heart motion, we used a respirator belt to restrict abdominal breathing, improve navigator efficiency and consequently shorten examination time. A β-blocker was taken orally by some patients to reduce heart rate. The two methods were effective to overcome the impact of breathing and heartbeat, improve the success rate of scanning, and

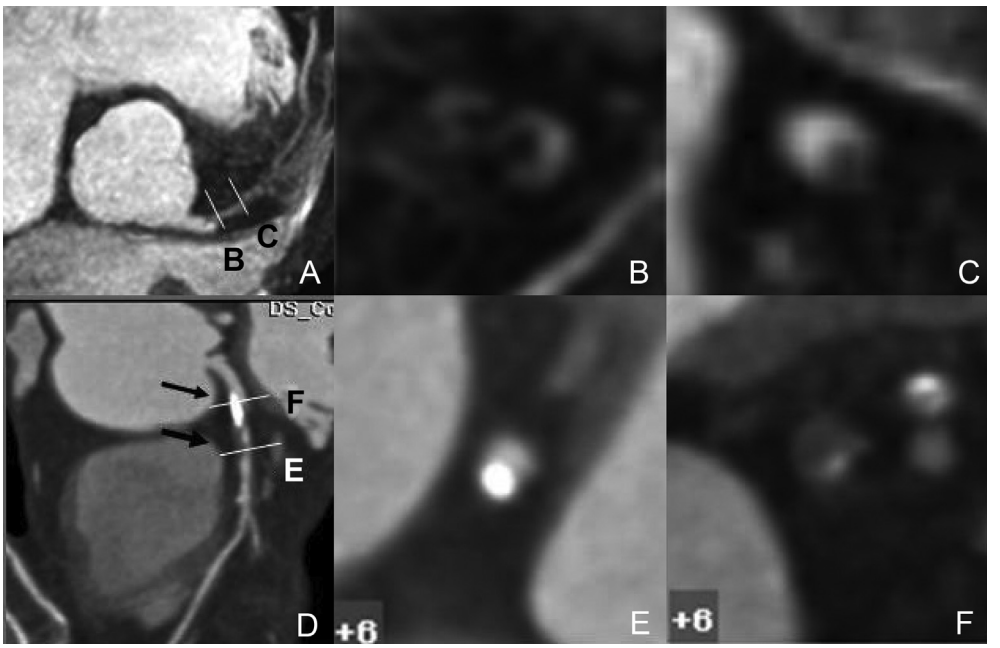


Fig. 2. Different types of coronary artery plaques. A: Coronary magnetic resonance angiography. D: Multidetector computed tomography (MDCT); Both show calcified plaque and non-calcified plaque (arrows) in the proximal segment of left anterior descending artery. B and C show the corresponding slices in MRI. The signal-to-noise ratio in the non-calcified plaque was significantly greater than that in the calcified plaque. E and F demonstrate the cross-section in calcified and non-calcified plaque slice of MDCT.

image quality. The success rate of scanning was up to 80%, which is considered acceptable for a clinical study with large sample size.

Our results indicated that the current black-blood coronary artery wall imaging technique could identify atherosclerotic plaques in the proximal and middle part of coronary artery. Despite insufficient spatial resolution, the result has clinical significance. Combination of MR black-blood and bright-blood coronary imaging technologies might be a better method for identification of coronary luminal stenosis. MRI is a non-invasive, radiation-free method for screening high-risk groups as well as for early detection of coronary atherosclerotic plaques and coronary artery disease. According to the Multi-Ethnic Study of Atherosclerosis (MESA) trial, the first to use this technology in clinical research on a large sample, black-blood coronary MR imaging was able to detect coronary remodeling in the high risk group.[8]

Collective results show that MRI can identify lipid, fiber, and hematoma in carotid artery plaque.[14–18] In our study, the spatial resolution of coronary plaque was $0.8 \times 1.1 \times 5$ mm, which was much larger than the spatial resolution of IVUS (in-plane resolution, 0.1 mm). However, the composition of coronary plaque could not be analyzed by only weighted imaging. Therefore, we roughly divided the coronary plaques into calcified, non-calcified, and mixed plaques; the results showed that the SNR in non-calcified plaque was significantly higher than calcified and mixed plaque. Thus, rather than analyzing the precise composition of coronary plaque as a whole, the current black-blood coronary artery wall imaging technology can be used to obtain information regarding plaque composition. Higher SNR of non-calcified plaques may be due to increased lipid content. The higher signal of calcified plaque as compared to normal wall, may be due to signals from other elements in the calcified plaque that are undetectable by current technology. MDCT was limited in identifying non-calcified plaque in lipid-rich plaques and fibrous plaques[4]; whether MRI can distinguish these two components of the plaque is an important issue that remains to be addressed.

## Conclusion

Coronary wall MRI can identify coronary plaques in the proximal and middle segments and has the potential to differentiate plaque types. Further technical advances, such as increasing the spatial resolution, multi-weighted imaging, and 3D coronary black-blood imaging will facilitate more extensive clinical application of this technology.

## Conflicts of interest

The authors declare that they have no competing interests.

## References

1. Virmani R, Kolodgie FD, Burke AP, Farb A, Schwartz SM. Lessons from sudden coronary death: a comprehensive morphological classification scheme for atherosclerotic lesions. *Arterioscler Thromb Vasc Biol*. 2000;20:1262–1275.
2. Falk E, Shah PK, Fuster V. Coronary plaque disruption. *Circulation*. 1995;92:657–671.
3. Davies MJ. A macro and micro view of coronary vascular insult in ischemic heart disease. *Circulation*. 1990;82(3 suppl 1):II38–46.
4. Sun J, Zhang Z, Lu B, et al. Identification and quantification of coronary atherosclerotic plaques: a comparison of 64-MDCT and intravascular ultrasound. *AJR Am J Roentgenol*. 2008 Mar;190:748–754.
5. Fayad ZA, Fuster V, Fallon JT, et al. Noninvasive in vivo human coronary artery lumen and wall imaging using black-blood magnetic resonance imaging. *Circulation*. 2000;102:506–510.
6. Botnar RM, Stuber M, Kissinger KV, Kim WY, Spuentrup E, Manning WJ. Noninvasive coronary vessel wall and plaque imaging with magnetic resonance imaging. *Circulation*. 2000;102:2582–2587.
7. Kim WY, Stuber M, Börnert P, Kissinger KV, Manning WJ, Botnar RM. Three-dimensional black-blood cardiac magnetic resonance coronary vessel wall imaging detects positive arterial remodeling in patients with nonsignificant coronary artery disease. *Circulation*. 2002;106:296–299.
8. Miao C, Chen S, Macedo R, et al. Positive remodeling of the coronary arteries detected by magnetic resonance imaging in an asymptomatic population mesa (multi-ethnic study of atherosclerosis). *J Am Coll Cardiol*. 2009;53:1708–1715.
9. Desai MY, Lai S, Barmet C, Weiss RG, Stuber M. Reproducibility of 3D free-breathing magnetic resonance coronary vessel wall imaging. *Eur Heart J*. 2005;26:2320–2324.
10. Maintz D, Ozgun M, Hoffmeier A, et al. Selective coronary artery plaque visualization and differentiation by contrast-enhanced inversion prepared MRI. *Eur Heart J*. 2006;27:1732–1736.
11. Bansmann PM, Priest AN, Muellerleile K, et al. MRI of the coronary vessel wall at 3 T: comparison of radial and cartesian k-space sampling. *AJR Am J Roentgenol*. 2007;188:70–74.
12. Kim WY, Astrup AS, Stuber M, et al. Subclinical coronary and aortic atherosclerosis detected by magnetic resonance imaging in type 1 diabetes with and without diabetic nephropathy. *Circulation*. 2007;115:228–235.
13. Macedo R, Chen S, Lai S, et al. MRI detects increased coronary wall thickness in asymptomatic individuals: the multi-ethnic study of atherosclerosis (MESA). *J Magn Reson Imaging*. 2008;28:1108–1115.
14. Cai JM, Hatsukami TS, Ferguson MS, Small R, Polissar NL, Yuan C. Classification of human carotid atherosclerotic lesions with in vivo multicontrast magnetic resonance imaging. *Circulation*. 2002;10:1368–1373.

15. Saam T, Hatsukami TS, Takaya N, et al. The vulnerable, or high-risk, atherosclerotic plaque: noninvasive MR imaging for characterization and assessment. *Radiology*. 2007;244:64−77.
16. Cai J, Hatsukami TS, Ferguson MS, et al. In vivo quantitative measurement of intact fibrous cap and lipid-rich necrotic core size in atherosclerotic carotid plaque: comparison of high-resolution, contrast enhanced magnetic resonance imaging and histology. *Circulation*. 2005;29:3437−3444.
17. Yuan C, Hatsukami TS, Cai J. MRI plaque tissue characterization and assessment of plaque stability. *Stud Health Technol Inform*. 2005;113:55−74.
18. Takaya N, Yuan C, Chu B, et al. Presence of intraplaque hemorrhage stimulates progression of carotid atherosclerotic plaques: a high-resolution magnetic resonance imaging study. *Circulation*. 2005;111:2768−2775.

Edited by Wei-Zhu Liu